Synergistic down-regulation of receptor tyrosine kinases by combinations of mAbs: Implications for cancer immunotherapy

Lilach M. Friedman*[†], Ariel Rinon[†‡], Bilha Schechter*, Ljuba Lyass[§], Sara Lavi[‡], Sarah S. Bacus[§], Michael Sela*, and Yosef Yarden[‡¶]

Departments of *Immunology and ‡Biological Regulation, The Weizmann Institute of Science, Rehovot 76100, Israel; and §Targeted Molecular Diagnostics, Westmont, IL 60559

mAbs to receptor tyrosine kinases such as EGF receptor/ErbB-1 and HER2/ErbB-2 inhibit the tumorigenic growth of certain cancer cells, but although recombinant versions of such Abs are already used in oncology wards, the mechanism underlying immunotherapy remains unknown. We report that anti-EGF receptor Abs promote a slow endocytic process distinct from the rapid EGF-induced receptor internalization. Combining mAbs that engage distinct epitopes significantly accelerates receptor degradation. In addition, mAb combinations are more effective than single Abs in inhibiting HER2 signaling *in vitro* and tumorigenesis in animals. We present a model attributing efficacy of immunotherapy to the size of Ab-receptor lattices formed at the cell surface, which dictates the rate of endocytic clearance and extent of signaling blockade.

ErbB | growth factor | oncogene | signal transduction | antibody

The four receptor tyrosine kinases of the ErbB family and their multiple ligand molecules form a layered signaling network, which is implicated in human cancer (reviewed in ref. 1): overexpression of ErbB-1/EGF receptor (EGFR) has been implicated as a feature of poor prognosis in various human malignancies. Moreover, deletion mutants of EGFR exist in brain tumors and point mutations have recently been reported in lung cancer (2). By contrast, ErbB-2/HER2 is rarely mutated in solid tumors. Instead, the *erbB-2* gene is frequently amplified in breast, ovarian, and lung cancer (3). Because of their oncogenic potential and accessibility, ErbB proteins have emerged as attractive targets for pharmaceutical interventions. One major strategy involves the use of mAbs. Early studies uncovered the tumor-inhibitory potential of mAbs directed at ErbB-1 and ErbB-2 (4, 5), and later studies indicated that anti-ErbB mAbs are effective when combined with various chemotherapeutic agents (6, 7). Indeed, the clinical benefit of combining mAbs with certain chemotherapeutic agents was notable, which led to the approval of mAbs to ErbB-2 (Herceptin) and EGFR (C225/Cetuximab) for the treatment of breast and colorectal cancer, respectively.

Two types of mechanisms have been implicated in ErbB-directed immunotherapy. The first involves mAb-mediated recruitment to tumors of natural killer cells through the Fc-γ activation receptors of these immune effector cells (8). The second type of mechanisms relates to intrinsic mAb activities, which include blockade of ligand binding or receptor heterodimerization (9), inhibition of downstream signaling to Akt (10), and acceleration of receptor internalization (11, 12). The latter mechanism is particularly attractive because ligand-induced endocytosis and degradation of active receptor tyrosine kinases (RTKs) is considered a major physiological process underlying attenuation of growth-promoting signals (13).

Several studies reported cooperative effects of mAb combinations (9, 12, 14–16), whereas others found that bivalent, Fc-lacking versions of anti-ErbB mAbs inhibit tumorigenic growth in animals (17, 18). These observations are difficult to explain in terms of a model attributing tumor inhibition solely to recruitment of immune cells. Hence, we addressed the possibility that mAb combinations better inhibit tumor growth because they effectively down-regulate RTKs. We conclude that the Ab-driven pathway of RTK internalization is distinct from ligand-induced endocytosis. Receptor entry into this pathway terminates signaling and its rate seems proportional to the size of Ab-ErbB lattices formed at the cell surface.

Materials and Methods

Materials. Unless indicated, materials were purchased from Sigma. Trastuzumab/Herceptin was provided by Genentech (South San Francisco, CA). Abs were purchased from Santa Cruz Biotechnology, except for anti-hemagglutinin (Roche, Basel, Switzerland).

Plasmid Transfections, Surface Biotinylation, and Immunoblotting. Plasmid transfections (1–2 μg of DNA per 90-mm plate) were performed by using the calcium phosphate or the Lipofectamine methods. For biotinylation, cells were first incubated with ligands or mAbs, which were then removed by using a low pH solution (0.15 M acetic acid/0.15 M NaCl; 4 min). Thereafter, cells were washed and incubated for 60 min at 4°C with *N*-hydroxysuccinimide-biotin (0.5 mg/ml; Calbiochem). Coupling of biotin was blocked with 15 mM glycine. The compositions of buffers, as well as the protocols for immunoprecipitation and immunoblotting were described (19).

Receptor Down-Regulation and mAb-Binding Assays. Cells were incubated at 37°C for different time periods in binding buffer containing EGF or mAb, rinsed, and surface-bound ligands removed, and the number of surface binding sites was determined by incubating the cells at 4°C with [^{125}I]EGF (5 ng/ml) for 1.5 h. For cross-competition assays, cells were treated at 4°C for 1 h with various concentrations of mAbs or EGF. Radiolabeled mAbs (8 nM) were then added, and the cells incubated for additional 15 min at 4°C before determination of radioactivity. All experiments were performed in triplicates and repeated thrice.

Assays Using a Reporter Gene. Cells were transfected with a reporter pSRE-Fluc plasmid containing the serum response element cloned upstream to the *c-fos* promoter and the luciferase gene (20). Twenty-four hours later, cells were incubated for 12 h at 37°C with various Abs in medium containing 0.1% serum.
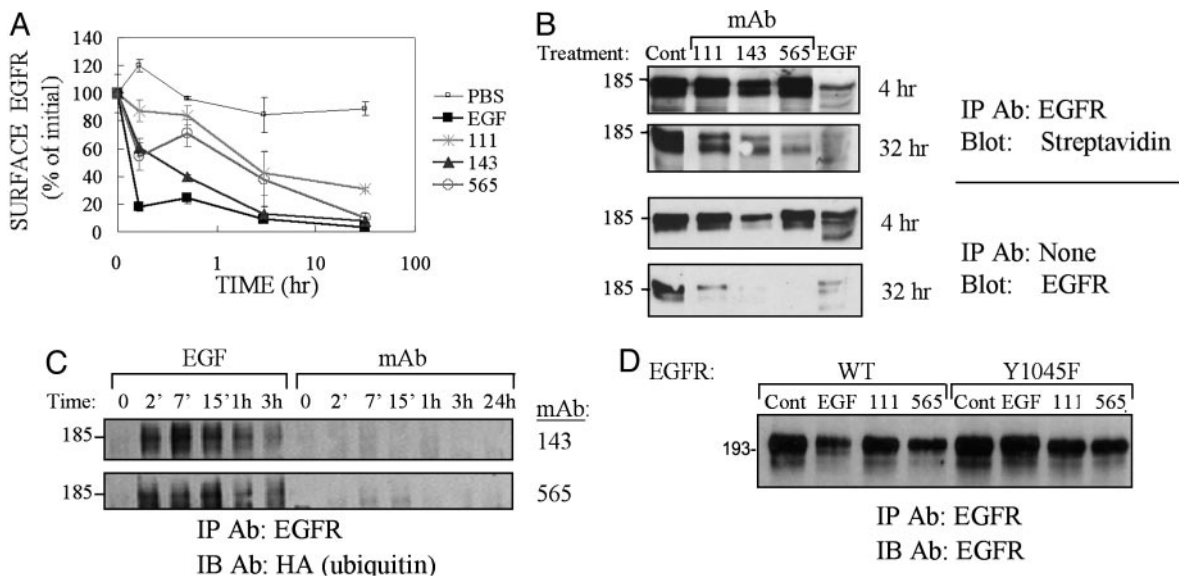
CELL BIOLOGY

Fig. 1. Down-regulation of EGFR by mAbs is independent of receptor ubiquitylation. (*A*) KB cells were treated with EGF (100 ng/ml) or mAbs (20 μg/ml) at 37°C for various time intervals. The cells were then washed and acid-stripped, and levels of surface receptor were determined (average ± SD) by using a radiolabeled EGF. (*B*) KB cells were treated as indicated for 4 or 32 h and washed as in *A*. This treatment was followed either by immunoblotting with an anti-EGFR Ab (*Lower*) or by surface biotinylation, followed by immunoprecipitation and blotting with streptavidin-horseradish peroxidase (*Upper*). (*C*) CHO cells transiently expressing EGFR, c-Cbl, and hemagglutinin-ubiquitin were incubated with EGF (100 ng/ml) or the indicated mAb (20 μg/ml) for various intervals. (*D*) CHO cells transiently expressing WT- or Y1045F-EGFR, along with c-Cbl, were incubated with EGF (100 ng/ml; 1 h), saline, or the indicated mAbs (10 μg/ml; 18 h). EGFR was analyzed after removal of bound ligands.

Then cells were stimulated 47 h later with Neu differentiation factor (NDF) (50 ng/ml) for 1 h at 37°C. Thereafter, cell extracts were prepared in a reporter lysis buffer (Promega), and after centrifugation (14,000 rpm for 15 min), 30-μl aliquots were incubated with 100 μl of luciferin buffer (0.1 M Tris-acetic acid/10 mM magnesium acetate/1 mM EDTA, pH 8.0/74 mM luciferin/2.2 mM ATP) and analyzed by using a luminator.

Generation of Abs. To generate mAbs to EGFR, we immunized mice with an IgB-1, a fusion protein containing the extracellular domain of EGFR fused to the Fc region of human IgG. Hybridomas were screened for inhibition of binding of a radio-labeled EGF to the surface of A-431 cells. Similarly, we generated a polyclonal Ab (pAb) to ErbB-2 by immunizing rabbits with IgB-2. The Ig fraction was purified by using a column of protein A.

Plasmid Construction. WT and Y1045F-EGFR vectors have been described (21). To construct ECD-glycosyl-phosphatidylinositol (GPI), we fused the GPI signal of the rat contactin-1 gene to the 3′ end of *erbB-2* cDNA (at nucleotide 2106). The extracellular domain-transmembrane (ECD-TM) was constructed by introducing a stop codon at nucleotide 2176.

Immunohistochemical Staining. A modified "Oil Red O in propylene glycol" method was used to visualize neutral lipids (22).

Immunofluorescence and Flow Cytometry. After treatment with mAbs, cells were fixed with paraformaldehyde (3%) and permeabilized in saline containing 1% albumin and 0.2% Triton X-100. Cells were then incubated for 30 min at 22°C with a Cy3-conjugated donkey-anti-mouse F(ab)₂ Ab. The coverslips were mounted in mowiol and examined with a Zeiss Axiovert confocal microscope. For flow cytometric analyses, cells were incubated for 1 h at 4°C in saline containing 0.1% albumin and FITC-conjugated 4D5 Ab (10 μg/ml) and then transferred to

37°C to allow internalization. Surface-bound mAbs were removed and cells resuspended and analyzed by flow cytometry to detect internalized mAbs. To determine background signals, cells were incubated with the mAb at 4°C and acid-stripped without transferring to 37°C.

Tumorigenic Cell Growth in Animals. Female CD/nude mice were s.c. injected with 3×10^6 N87 human gastric cancer cells overexpressing ErbB-2. Abs were injected i.p. at days 3, 7, and 10. Groups of four mice were used; each received 0.6 mg of mAb. Tumor parameters were measured twice weekly, and tumor volume was calculated.

Results

Anti-EGFR Abs Induce Slow, Ubiquitylation-Independent Receptor Down-Regulation. To compare EGF- and mAb-induced receptor down-regulation, we generated a series of three mAbs, which were selected for their ability to displace cell surface-bound EGF molecules. Ab-induced down-regulation of EGFR was evaluated in KB cells treated with EGF or mAbs. Whereas internalization induced by EGF removed most (80%) receptors within 10 min, the three mAbs induced significantly slower endocytosis (Fig. 1*A*). To directly assess EGFR internalization, we surface-labeled cells with biotin after incubation with mAbs or EGF (Fig. 1*B*). This experiment confirmed that mAbs slowly internalize and degrade EGFR (Fig. 1*B*).

The robustness of EGF-induced down-regulation is attributed to c-Cbl-mediated conjugation of ubiquitin to EGFR (reviewed in ref. 13). To test ubiquitylation we used CHO cells ectopically expressing EGFR, c-Cbl, and hemagglutinin-ubiquitin. Unlike EGF-treated cells, cells treated with mAb111 or mAb565 displayed faint, if any ubiquitylation of EGFR (Fig. 1*C*). Next, we used a mutant form of EGFR, Y1045F, which cannot directly recruit c-Cbl (21). Although the mutant receptor displayed resistance to EGF-induced degradation, it underwent nearly normal down-regulation in response to treatment with mAbs
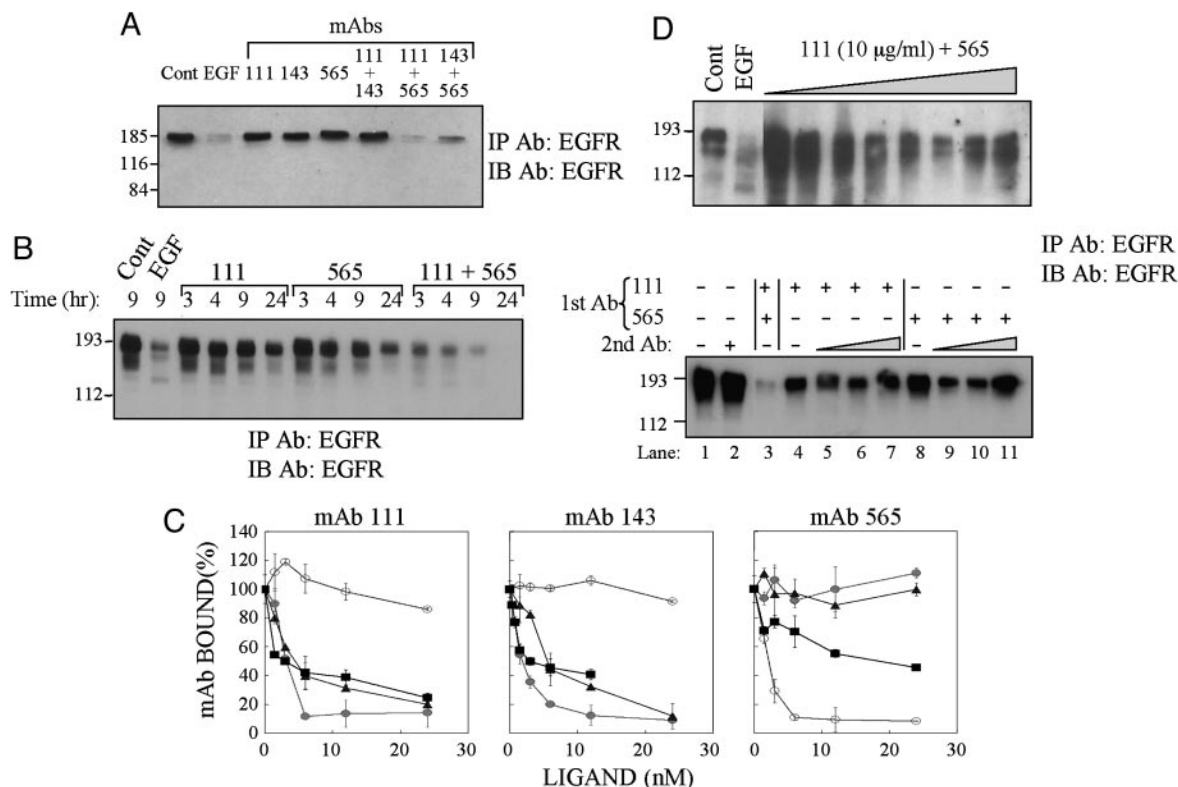
Fig. 2. Combinations of anti-receptor mAbs down-regulate EGFR better than each mAb alone. (*A*) KB cells were treated for 13 h with EGF (100 ng/ml) or the indicated mAbs (total: 20 μg/ml). Cell extracts were analyzed after stripping of bound ligands. (*B*) KB cells were treated for various time intervals and extracts analyzed as in *A*. (*C*) KB cells were treated for 1 h at 4°C with mAbs 111 (●), 143 (▲), 565 (○), or EGF (■). The indicated radiolabeled mAbs (8 nM) were then added, and the cells were incubated for an additional 15 min before determination of radioactivity. (*D Upper*) KB cells were treated for 18 h with saline (Cont) or EGF (100 ng/ml) or cotreated with mAbs 111 (10 μg/ml) and 565 (2.5–20 μg/ml). (*D Lower*) KB cells were preincubated with saline, EGF (100 ng/ml), or the indicated mAbs (total: 10 μg/ml) for 3 h at 4°C. The medium of all cells (except lane 3) was then replaced with fresh medium containing a goat anti-mouse IgG [second Ab: either 40 (+) or 10, 20, and 40 μg/ml], and cells were incubated for additional 18 h at 37°C.

(Fig. 1*D*). In conclusion, mAb-induced degradation of EGFR is slow relative to the effect of EGF, and unlike the ligand-induced process, Cbl-mediated ubiquitylation may not be involved.

Combinations of Anti-Receptor mAbs Directed at Distinct Epitopes Better Down-Regulate EGFR than each mAb Alone. In an attempt to increase efficacy of down-regulation, we tested mAb combinations (Fig. 2*A*). Although each mAb induced limited down-regulation after a 13-h incubation, two mAb combinations dramatically increased receptor degradation. Down-regulation of EGFR by the more effective combination was not only more extensive than each Ab alone, but also evolved more rapidly (Fig. 2*B*). To understand why certain combinations are more effective, we performed cross-competition analyses by using radiolabeled mAbs (Fig. 2*C*). The results confirmed that each mAb is displaceable by an unlabeled EGF and showed that the nonsynergistic mAbs are cross-competitive, whereas Abs of the synergistic combinations bind distinct epitopes.

Because mAbs that share binding sites form EGFR dimers, whereas combinations of Abs recognizing distinct epitopes will form larger lattices, we assumed that the rate of EGFR removal from the cell surface is proportional to the size of antigen-Ab lattices. Two predictions raised by this model were experimentally tested. First, lattices are expected to dissociate at very high Ab concentrations because of monovalent binding to EGFR. Indeed, when the concentration of mAb565 was gradually increased, the extent of EGFR degradation after co-incubation with mAb111 displayed a bell-shaped pattern (Fig. 2*D*). Secondly, when surface-bound mAbs were aggregated with a sec-

ondary anti-mouse IgG, we observed an increase in EGFR degradation (Fig. 2*D Lower*). As expected, the efficacy of down-regulation was reduced at high concentrations of the secondary Ab. In conclusion, our results support the possibility that antireceptor Abs drive internalization and subsequent degradation of EGFR in a mechanism that involves formation at the cell surface of Ab-receptor complexes analogous to the well characterized precipitin reaction occurring in solution.

Down-Regulation of ErbB-2 by a Combination of mAbs Is Dynamin-Dependent but Requires no Cytoplasmic Receptor's Portions. To extend our observations to ErbB-2, we selected a combination of two Abs: L26, which inhibits heterodimerization of ErbB-2 (9), and Herceptin (23). A cell surface-bound L26 could not be displaced by a large molar excess of Herceptin, and L26 did not affect Herceptin binding (Fig. 3*A*). As expected, a 6-h treatment with a mixture of these mAbs resulted in a close to complete disappearance of ErbB-2, but neither mAb alone significantly down-regulated ErbB-2 at this time point (Fig. 3*B*). To test the prediction that a polyvalent Ab would induce extensive down-regulation, we raised a rabbit pAb to ErbB-2 and tested effects on receptor turnover. As predicted, the pAb extensively down-regulated ErbB-2 (Fig. 3*B*). Two additional tests confirmed the ability of mAbs to enhance endocytosis. First, using a fluorescent 4D5 (the parental form of Herceptin) and an unlabeled L26, we detected robust intracellular accumulation of the fluorescent mAb when cells were co-incubated with the other Ab (Fig. 3*C*). Likewise, confocal microscopy that followed the fate of cell-
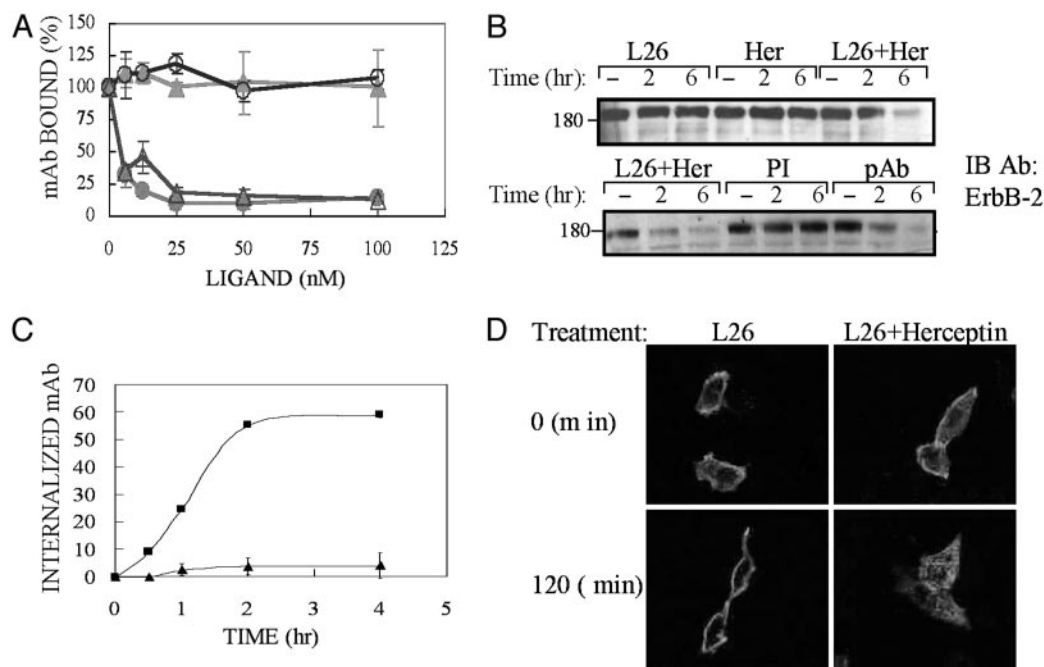
CELL BIOLOGY

Fig. 3. Combinations of mAbs down-regulate ErbB-2 better than each mAb alone. (*A*) SKBR-3 cells were treated for 1 h with various concentrations of mAbs L26 (circles) or Herceptin (triangles) at 4°C. Radiolabeled mAbs L26 (8 nM; filled symbols) or Herceptin (open symbols) were then added, and the cells were incubated for 15 min. After washing, radioactivity was measured and expressed as average ± SD. (*B*) HEK-293T cells (*Upper*) ectopically expressing ErbB-2 or T47D cells (*Lower*) were treated with L26 and/or Herceptin (Her; total: 20 µg/ml) at 37°C for the indicated time intervals. PI, preimmune Abs. (*C*) SKBR-3 cells were treated at 37°C for the indicated time intervals with fluorescein-labeled 4D5-mAb (10 µg/ml) in the absence (▲) or presence (■) of L26-mAb. Thereafter, cells were washed and acid-stripped, and internalized 4D5 was determined by using a cell sorter. (*D*) CB2 cells were incubated with a mixture of L26 and Herceptin (20 µg/ml each) or L26 alone (40 µg/ml) at 37°C for the indicated time periods. Thereafter, cells were washed, fixed, and permeabilized, and ErbB-2 was detected by using confocal microscopy with a Cy3-conjugated anti-mouse IgG.

bound L26 by using a secondary Ab revealed enhanced endocytosis of L26 when combined with Herceptin (Fig. 3*D*).

To address the mechanism underlying endocytosis of ErbB-2, we examined dependence on dynamin, a GTPase regulating the "pinching off" of endocytic vesicles at the plasma membrane (24). It has previously been shown that a dominant-negative form of dynamin (K44A) blocks EGF endocytosis (24). Hence, we first confirmed the effects of WT and K44A on EGF-induced down-regulation of EGFR. When ectopically expressed, along with EGFR and c-Cbl, K44A inhibited EGF-induced degradation of EGFR and enhanced receptor expression (Fig. 4*A*). When

applied to ErbB-2, K44A almost abolished receptor down-regulation upon treatment of cells with a combination of mAbs (Fig. 4*A Lower*).

Having established involvement of dynamin in mAb-induced receptor down-regulation, we next addressed structural requirements. To this end we constructed two mutants, which are schematically presented in Fig. 4*B*. ECD-TM is an ErbB-2 molecule that lacks the entire cytoplasmic domain, whereas ECD-GPI is a lipid-anchored full extracellular domain of ErbB-2. When electrophoresed, both mutants displayed two bands corresponding to 120 and 135 kDa (Fig. 4*C Lower*).
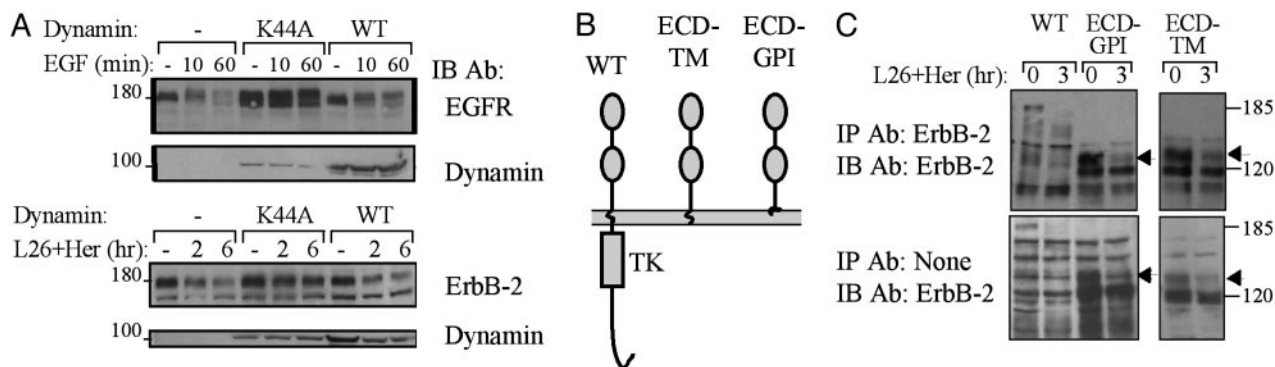

Fig. 4. Down-regulation of ErbB-2 by combinations of mAbs is dynamin-dependent but requires no cytoplasmic or transmembrane portions of ErbB-2. (*A*) HEK-293T cells were cotransfected with plasmids encoding EGFR (*Upper*) or ErbB-2 (*Lower*), along with plasmids encoding c-Cbl and dynamin (WT or K44A). After 48 h, cells were treated with EGF (100 ng/ml) or a combination of L26 and Herceptin (Her; total: 20 µg/ml), and extracts were analyzed. (*B*) A diagram of ErbB-2 molecules analyzed, either WT, a mutant lacking the cytoplasmic domain (ECD-TM), or the full ectodomain fused to a GPI-attachment signal (ECD-GPI). (*C*) CHO cells were treated for 3 h with a mixture of mAbs L26 and Herceptin (5 µg/ml each). Note that only the surface-localized forms of ECD-GPI and ECD-TM (arrows) were affected by mAbs.
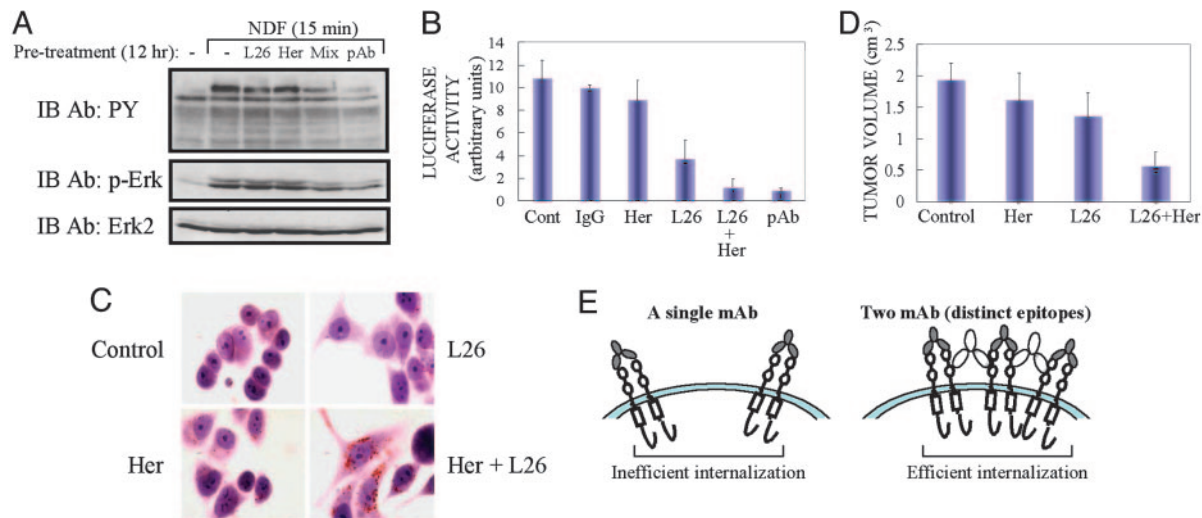
Fig. 5. Combinations of anti-ErbB-2 Abs inhibit growth factor signaling, promote differentiation, and reduce tumor growth. (*A*) T47D cells were incubated for 12 h with mAbs (total: 10 μg/ml), including a mixture (mix) of L26 and Herceptin (Her). Cells were then washed and stimulated with NDF (50 ng/ml) for 15 min, and cell extracts were analyzed. (*B*) MCF-7 cells were transfected with a *fos* reporter plasmid, and, 24 h later, cells were split and incubated for 12 h with the indicated Abs, including a control human IgG. Later (47 h), cells were washed and stimulated for 1 h with NDF (50 ng/ml), followed by analysis by using a luminator. (*C*) AU-565 cells were treated for 3 d with mAbs (30 μg/ml) and then stained for neutral lipids. (*D*) CD-1/nude mice were injected s.c. with 3×10^6 N87 cells. mAbs (600 μg per animal) were injected i.p. 3, 7, and 10 d later. Saline-injected mice were used for control. Tumor volumes were measured after 18 d, and the mean volume of each group of four mice was plotted. The difference between treatments with each mAb alone and their combination is statistically significant ($P < 0.05$). (*E*) A model comparing the size of ErbB-Ab complexes formed at the cell surface by one or two mAbs. We propose that the rate of internalization is proportional to the size of surface-associated antigen-Ab lattices.

Surface biotinylation experiments revealed that only the 135-kDa species reached the plasma membrane, and analysis of sensitivity to endoglycosidase H indicated that maturation of the nascent 120-kDa species was defective (data not shown). In accordance, only the 135-kDa forms of ECD-TM and ECD-GPI underwent down-regulation upon treatment of cells with a mixture of mAbs (Fig. 4*C*). Taken together, these observations indicate that no cytoplasmic or transmembrane motifs of ErbB-2 are necessary for mAb-induced internalization and degradation.

Cooperative Inhibition of Signaling and Tumor Growth by Polyvalent Ab Binding to ErbB-2. Because ErbB-2 acts as a ligand-less coreceptor that augments growth factor signaling, Ab mixtures capable of down-regulation are expected to desensitize ErbB signaling. To test this model, we concentrated on the mitogen-activated protein kinase (Erk) pathway and the corresponding nuclear outcome, namely transcription from promoters containing the serum response element (20). Treatment of T47D mammary tumor cells with NDF resulted in rapid stimulation of ErbB phosphorylation on tyrosine residues and activation of Erk (Fig. 5*A*). Significant signal reduction was observed in cells pretreated with mixtures of anti-ErbB Abs, either a combination of two mAbs or a rabbit pAb. In addition, by using a reporter gene we found that transcription from the serum response element was stimulated 8- to 12-fold by NDF, but pretreatment with Ab mixtures, unlike Herceptin alone or a control Ig, almost completely blocked transcription (Fig. 5*B*).

Treatment with mAbs to ErbB-2 transforms mammary tumor cells into well differentiated flat cells, which synthesize neutral lipids (22). To examine possible Ab synergy on induction of mammary differentiation, we incubated cells with Herceptin, L26, or a combination and stained for neutral lipids 4 d later. The results demonstrate that each mAb is capable of inducing a differentiated phenotype, but a mixture of mAbs was significantly more effective (Fig. 5*C*), in line with more extensive down-regulation of ErbB-2. Because previous studies related enhanced endocytosis of ErbB-2 to reduced tumorigenesis (9,

12), these cooperative effects raised the possibility that L26 and Herceptin will augment each other's ability to retard tumors. To test this prediction, we injected mice with N87 gastric cancer cells overexpressing ErbB-2. Animals were injected with mAbs or their combination 3, 7, and 10 d later. Fig. 5*D* presents the results recorded at day 18. At this early time point, both L26 and Herceptin only partially inhibited tumor growth (30% and 17% inhibition, respectively), but their combination yielded a 70% reduction in tumor volume ($P < 0.05$). In conclusion, a combination of anti-ErbB-2 mAbs that engage distinct epitopes synergistically inhibited the tumorigenic growth of ErbB-2-driven cancer cells, in line with enhanced ability of the mixture to down-regulate ErbB-2 and block growth factor signaling.

Discussion

Elucidating mechanisms underlying immunotherapy directed at oncogenic RTKs may enable enhancing the commonly weak therapeutic efficacy, as well as overcoming inherent and acquired resistance. Previous studies performed with various animal models raised the possibility that combining anti-ErbB-2 mAbs will increase the therapeutic potential, but the mechanism remained unknown (9, 12, 14, 15, 25, 26). The present study extends the cooperative effects to EGFR, reveals that synergy requires binding to distinct epitopes, and shows that the cooperative action of mAb combinations includes early (Fig. 5*A*), as well as long-term cellular effects (Fig. 5 *B* and *C*). More important, our results offer a model attributing immunotherapy to the ability of Abs to internalize and degrade receptor molecules.

Fig. 5*E* outlines the proposed model. Accordingly, because of their bivalence, mAbs are able to form receptor homodimers, but treatment with combinations of mAbs will generate much larger receptor-Ab complexes. For several reasons we propose that the rate of endocytosis of mAb-RTK complexes is proportional to their size, in analogy to the entry of viruses and other polyvalent ligands and pathogens. Firstly, both mAb combinations and a pAb (Fig. 3*B*) induce earlier (Fig. 2*B*) and more extensive

receiver internalization. Secondly, the observed bell-shaped dose–response (Fig. 2D), as well as the ability of a secondary Ab to increase receptor degradation (Fig. 2D), may be interpreted in terms of a precipitin reaction occurring at the cell surface. Thirdly, the strict dependence of mAb cooperation on simultaneous engagement of more than one epitope (Figs. 2C and 3A), in line with previous reports (15, 25), is compatible with the notion that large surface aggregates internalize faster than smaller complexes.

Ab-induced internalization may be as robust as ligand-mediated endocytosis of EGFR (Fig. 2B), but the underlying mechanisms significantly differ: Unlike rapid EGF-induced endocytosis, mAb-induced homodimers undergo relatively slow endocytosis, which involves only weak ubiquitylation (Fig. 1). In addition, unlike the ligand-induced pathway, mAb-induced internalization requires no cytoplasmic receptor's determinants. Nevertheless, both pathways require dynamin (Fig. 4A), raising the question: Which internalization pathway is used by mAbs? Presumably, mAbs with agonistic activity recruit the Cbl protein and thereby increase receptor ubiquitylation, as we reported (19). This inducible pathway likely sorts receptors to clathrin-coated pits, but it plays only a secondary role in mAb-induced internalization. The following considerations suggest that mAb-induced internalization instigates primarily in caveolin-coated

membrane domains: EGFR localization to caveolae requires no cytoplamic motifs (27), in line with the ability of mAbs to enhance degradation of a mutant ErbB-2 containing no intracellular tail (ECD-TM, Fig. 4C); the lipid anchor of ECD-GPI is expected to direct the internalization-competent fusion protein to caveolae; and dynamin, which is necessary for mAb-induced internalization of ErbB-2 (Fig. 4A), is known to be involved in caveolar endocytosis.

In summary, by addressing the cooperative ability of certain mAbs to inhibit tumors, our study proposes Ab-induced down-regulation of growth factor receptors as a candidate mechanism of immunotherapy. Consistent with this notion, EGF-induced down-regulation of EGFR is considered a critical mechanism of signal attenuation (13). Further, the model we propose offers strategies to enhance the therapeutic efficacy of clinically approved Abs such as Herceptin and C225/Cetuximab. Along with testing the clinical implications of our findings, future studies will address possible interactions between the Fc portions of therapeutic mAbs and the caveolae/raft-associated endocytic machinery.

1. Yarden, Y. & Sliwkowski, M. X. (2001) *Nat. Rev. Mol. Cell Biol.* **2,** 127–137.
2. Lynch, T. J., Bell, D. W., Sordella, R., Gurubhagavatula, S., Okimoto, R. A., Brannigan, B. W., Harris, P. L., Haserlat, S. M., Supko, J. G., Haluska, F. G., *et al.* (2004) *New Engl. J. Med.* **350,** 2129–2139.
3. Slamon, D. J., Godolphin, W., Jones, L. A., Holt, J. A., Wong, S. G., Keith, D. E., Levin, W. J., Stuart, S. G., Udove, J., Ullrich, A., *et al.* (1989) *Science* **244,** 707–712.
4. Drebin, J. A., Stern, D. F., Link, V. C., Weinberg, R. A. & Greene, M. I. (1984) *Nature* **312,** 579–588.
5. Masui, H., Kawamoto, T., Sato, J. D., Wolf, B., Sato, G. & Mendelsohn, J. (1984) *Cancer Res.* **44,** 1002–1007.
6. Aboud-Pirak, E., Hurwitz, E., Pirak, M. E., Bellot, F., Schlessinger, J. & Sela, M. (1988) *J. Natl. Cancer Inst.* **80,** 1605–1611.
7. Pietras, R. J., Pegram, M. D., Finn, R. S., Maneval, D. A. & Slamon, D. J. (1998) *Oncogene* **17,** 2235–2249.
8. Clynes, R. A., Towers, T. L., Presta, L. G. & Ravetch, J. V. (2000) *Nat. Med.* **6,** 443–446.
9. Klapper, L. N., Vaisman, N., Hurwitz, E., Pinkas-Kramarski, R., Yarden, Y. & Sela, M. (1997) *Oncogene* **14,** 2099–2109.
10. Yakes, F. M., Chinratanalab, W., Ritter, C. A., King, W., Seelig, S. & Arteaga, C. L. (2002) *Cancer Res.* **62,** 4132–4141.
11. Maier, L. A., Xu, F. J., Hester, S., Boyer, C. M., McKenzie, S., Bruskin, A. M., Argon, Y. & Bast, R. C., Jr. (1991) *Cancer Res.* **51,** 5361–5369.
12. Hurwitz, E., Stancovski, I., Sela, M. & Yarden, Y. (1995) *Proc. Natl. Acad. Sci. USA* **92,** 3353–3357.
13. Marmor, M. D. & Yarden, Y. (2004) *Oncogene* **23,** 2057–2070.
14. Kasprzyk, P. G., Song, S. U., Di Fiore, P. P. & King, C. R. (1992) *Cancer Res.* **52,** 2771–2776.
15. Spiridon, C. I., Ghetie, M. A., Uhr, J., Marches, R., Li, J. L., Shen, G. L. & Vitetta, E. S. (2002) *Clin. Cancer Res.* **8,** 1720–1730.
16. Stancovski, I., Hurwitz, E., Leitner, O., Ullrich, A., Yarden, Y. & Sela, M. (1991) *Proc. Natl. Acad. Sci. USA* **88,** 8691–8695.
17. Fan, Z., Lu, Y., Wu, X. & Mendelsohn, J. (1994) *J. Biol. Chem.* **269,** 27595–27602.
18. Xu, F., Lupu, R., Rodriguez, G. C., Whitaker, R. S., Boente, M. P., Berchuck, A., Yu, Y., DeSombre, K. A., Boyer, C. M. & Bast, R. C., Jr. (1993) *Int. J. Cancer* **53,** 401–408.
19. Klapper, L. N., Waterman, H., Sela, M. & Yarden, Y. (2000) *Cancer Res.* **60,** 3384–3388.
20. Johansen, F. E. & Prywes, R. (1994) *Mol. Cell. Biol.* **14,** 5920–5928.
21. Waterman, H., Katz, M., Rubin, C., Shtiegman, K., Lavi, S., Elson, A., Jovin, T. & Yarden, Y. (2002) *EMBO J.* **21,** 303–313.
22. Bacus, S. S., Gudkov, A. V., Zelnick, C. R., Chin, D., Stern, R., Stancovski, I., Peles, E., Ben Baruch, N., Farbstein, H., Lupu, R., *et al.* (1993) *Cancer Res.* **53,** 5251–5261.
23. Carter, P., Presta, L., Gorman, C. M., Ridgway, J. B., Henner, D., Wong, W. L., Rowland, A. M., Kotts, C., Carver, M. E. & Shepard, H. M. (1992) *Proc. Natl. Acad. Sci. USA* **89,** 4285–4289.
24. Damke, H., Baba, T., Warnock, D. E. & Schmid, S. L. (1994) *J. Cell Biol.* **127,** 915–934.
25. Harwerth, I. M., Wels, W., Schlegel, J., Muller, M. & Hynes, N. E. (1993) *Br. J. Cancer* **68,** 1140–1145.
26. Drebin, J. A., Link, V. C. & Greene, M. I. (1988) *Oncogene* **2,** 273–277.
27. Yamabhai, M. & Anderson, R. G. (2002) *J. Biol. Chem.* **277,** 24843–24846.